RE-EVALUATION OF CONTROL PERFORMANCE FOR TURBULENT SKIN FRICTION DRAG REDUCTION IN TERMS OF ENERGY SAVING AND CONVENIENCE

Y. Hasegawa[1,2], *B. Frohnapfel*[1,3] *and M. Quadrio*[4]

[1] *Center of Smart Interfaces, TU Darmstadt, Germany*
[2] *Department of Mechanical Engineering, The University of Tokyo, Japan*
[3] *Institute of Fluid Mechanics, Karlsruhe Institute of Technology, Germany*
[4] *Dipartimento di Ingegneria Aerospaziale del Politecnico di Milano, Italy*

hasegawa@csi.tu-darmstadt.de

Abstract

Flow control techniques for turbulent drag reduction in internal flows are typically evaluated under two alternative flow conditions, i.e. at constant mass flow rate or constant pressure gradient. Succesfull control leads to reduction of drag and pumping power at constant mass flow rate, whereas constant pressure gradient leads to an increase of the mass flow rate and pumping power. In practical applications, however, a compromise between the energy consumption and the corresponding convenience (flow rate) achieved with that amount of energy has to be reached so as to accomplish a goal which in general depends on the specific application. Based on this idea, we describe the derivation of two dimensionless parameters which quantify the total energy consumption and the required time (convenience) for transporting a given volume of fluid through a given duct. Performances of existing drag reduction strategies are re-evaluated within the present framework.

1 Introduction

Flow control with the goal of reducing the skin friction drag on the fluid-solid interface is an active fundamental research area, motivated by its potential for significant energy savings and reduced emissions in the transport sector. Up to now, various drag-reducing techniques, applied to the classic turbulent channel or pipe flows, have been studied mainly through Direct Numerical Simulation (DNS) of the Navier–Stokes equations, and their control performance has been evaluated while keeping constant in time either the flow rate (CFR) or – less often – the pressure gradient (CPG).

Under the CFR condition, a successful drag-reducing technique effectively reduces friction drag, which immediately translates into a reduction of the pumping energy. The CPG condition, on the other hand, has the advantage of keeping the friction-based Reynolds number unchanged by design. As a consequence, friction drag is unchanged too, and drag reduction manifests itself through an increase of the flow rate, which implies an increase in the power required to drive the flow.

In the present problem, two main factors are at play: flow rate and pressure gradient. The flow rate, constant in the CFR approach, is an essential consequence of employing a duct to transport a given amount of fluid through the duct itself over a certain distance, and we term it *convenience*. The pressure gradient, constant in the CPG approach, is directly related to the *energy consumption* required to achieve that convenience. In real-life applications using flow control, minimizing energy consumption for a given flow rate (the CFR approach) and maximizing convenience for a fixed energy consumption (the CPG approach) are only two of the many possible strategies conceivable to balance the two intervening factors. In general, the designer of a fluidic system would consider both convenience and energy requirements, the relative value and cost of which will depend on the specific application. The optimal use of a control technique is the one that achieves maximum value at minimum cost, as determined by the designer.

In the present study, we develop a unified framework to assess (non necessarily active) flow control techniques against whatever application-dependent value-for-money considerations will be possible. A new evaluation plane is proposed in which both quantities, i.e. energy consumption and convenience (or, in other words, money and time), are simultaneously and explicitly considered. This new plane can be viewed as an improved version of the familiar $C_f - Re$ plane, which describes in a dimensionless way how the flow rate and the pressure gradient required to achieve that flow rate are related. In the new plane, an analogous non-dimensional description relates the flow rate and the energy expenditure required to achieve that flow rate, possibly including control energy. Re-evaluating existing drag-reduction data by taking advantage of this plane will give us new insight on their perfor-

mance and on the way we have to go for flow control techniques to become reality in applications.

2 Dimensional Analysis

Energy-Convenience Map

We shall consider a given fluid volume V_f^* which has to be transported through a duct by means of a pressure gradient. The asterisk represents dimensional quantities throughout this paper. The flow is assumed to be fully developed. The cross sectional area A^* and the wetted perimeter C^* of the duct do not vary along the streamwise direction x. The hydraulic diameter is defined as $D^* = 4A^*/C^*$.

A simple analysis leads to the following relationship for the pumping energy per unit wetted area:

$$E_p^* = \tau_w^* \frac{V_f^*}{A^*} = \frac{M^* {U_b^*}^2 C_f}{2A^*}, \tag{1}$$

where τ_w^*, U_b^*, ρ and $M^* = \rho^* V_f^*$ are the wall-shear-stress, the bulk mean velocity, the fluid density and the total mass of the transported fluid, respectively. The dimensionless friction coefficient C_f is defined as

$$C_f = \frac{\tau_w^*}{\frac{1}{2}\rho^* {U_b^*}^2}, \tag{2}$$

In order to evaluate control performance in terms of energy consumption and convenience, we start from the plot sketched in Fig. 1 (a), where the vertical axis is pumping energy E_p^* (and thus degree of energetic cost), and the horizontal axis is $1/U_b^*$, which represents the time for a fluid to travel over a unit length (and thus the degree of convenience). In a laminar flow $C_f \propto {U_b^*}^{-1}$ so that $E_p^* \propto U_b^*$, which is plotted as a dashed line in Fig. 1 (a). In non-controlled turbulent flows, the Blasius correlation (Schlichting, 1979) can be employed, from which $C_f \propto {U_b^*}^{-1/4}$ and $E_p^* \propto {U_b^*}^{7/4}$, which is depicted by a solid line in Fig. 1 (a). The objective of turbulence control is to achieve a flow state located in the region left/below the solid line. This plot naturally emphasizes that reduced energy consumption can easily be achieved when one is willing to sacrifice convenience, i.e. wait longer for a certain amount of fluid to arrive, and that high convenience, i.e. extremely fast transport, increases the energy requirements significantly.

Now, we suppose to apply control to the non-controlled flow state N in Fig. 1 (a). When U_b^* is kept constant (CFR), the control shifts N along the vertical arrow to, say, A. The reduction of E_p^*, i.e. the distance $|NA|$ between points N and A, is equivalent to drag reduction. On the other hand, under the CPG condition, Eqn. (1) indicates that E_p^* also remains constant, since τ_w is unchanged: in this case, successful control shifts N to the left along the horizontal arrow to B.

The dash-dotted line connecting the origin and flow state N represents the points for which the pumping *power*, i.e. the pumping energy divided by the operating time, remains constant. A shift to point C along the arrow in Fig. 1 (a) therefore corresponds to a controlled state that requires the same power input as the non-controlled state (constant power input, CPI): if flow control is succesful, such a state provides at the same time larger flow rate and smaller pumping energy.

If the flow control technique is of the active type and thus requires energy to operate, its energy input E_c^* must enter the picture. In order to account for E_c^*, Fig. 1 (a) with just pumping energy E_p^* is replaced by Fig. 1 (b), where the total energy $E_t^* = E_p^* + E_c^*$ is used on the vertical axis. The paths for a controlled flow state under constant flow rate and constant pressure gradient are shown by the arrows NA' and NB'. The solid and broken lines for non-controlled turbulent and laminar flows are the same as those in Fig. 1 (a), since $E_t^* = E_p^*$. The additional control energy input E_c^* is reflected in Fig. 1 (b) by the shift of points A and B in the vertical direction to A' and B', respectively. According to Bewley (2009) and Fukagata et al. (2009), the total energy consumption at a given flow rate is minimized when the flow becomes laminar. Therefore, no flow state can be located below the laminar curve, i.e., in the grey region in Fig. 1 (b). We also note that, in analogy to Fig. 1 (a), a line connecting the origin in Fig. 1 (b) and any point along the non-controlled curve represents flow states with the same total power consumption (CPI).

Implementation of Cost Function

The plane depicted in Fig. 1 (b) shows that several paths are possible to move the flow state from the non-controlled point N towards the laminar curve. The three particular ones considered so far, i.e. the CFR, CPG and CPI straight lines, are not the only ones, and not necessarily the best ones: only application-specific considerations allow the designer to rank the various strategies. The energy-convenience plane is a natural workspace where the chosen strategy can be represented in terms of an application-dependent cost function $\mathcal{F} = \mathcal{F}(E_t^*, U_b^*)$ to be minimized.

Three energy-convenience maps with typical cost functions are shown in Fig. 2 (a) - (c). The dotted lines represent the isolines of each cost function. The minimization is first constrained by the maximum affordable energy expenditure $(E_t^*)_{max}$ and by the maximum affordable inconvenience $(1/U_b^*)_{max}$. This avoids a trivial solution such as $U_b^* = 0$ or $E_t^* = \infty$ when the cost function includes only one of the two competing factors, i.e., E_t^* and U_b^*. An admissible region bounded by a dashed line in Fig. 2 is consequently defined, and the optimal flow state should exist either inside the region or on its boundary.

The case where $\mathcal{F} = E_t^*$ as shown in Fig. 2 (a) is considered first. When control is not applied, only the flow states on the uncontrolled turbulent curve are realizable. In this case, point N shown in Fig. 2 a) provides the minimum value of $\mathcal{F}$, and is therefore op-

timal. The downward arrow from point N shows the local gradient of $\mathcal{F}$, indicating that a control strategy changing the flow state in this direction is most effective to decrease the objective function. This particular choice of $\mathcal{F}$ corresponds to the CFR condition. Since flow states below the laminar curve cannot be realized, the lower-bound of $\mathcal{F}$ is obtained at point X on the laminar curve.

Similarly, when $\mathcal{F} = 1/U_b^*$, the optimal flow state without control is given by the intersection point N of the turbulent curve and the upper boundary of the admissible region as shown in Fig. 2 (b). In this case, the local gradient of $\mathcal{F}$ indicates that enhancing U_b^* under the constant E_t^* is the optimal strategy. If the applied control is passive or E_c^* in active control is negligibly small, E_t^* is equivalent to E_p^*, so that the optimal control strategy results in the CPG condition. Again, the minimum $\mathcal{F}$ is achieved at point X on the boundary of the admissible region.

As a less obvious example, Fig. 2 c) shows isolines of $\mathcal{F} = (E_t^*)^2 + (1/U_b^*)^2$, where the energy saving and the convenience are considered to be equally important. The optimal flow state N without control, as well as the optimal state X with control, are located inside the admissible region; the local gradient of $\mathcal{F}$ is always pointing towards the origin, indicating that the control under the CPI condition is locally the optimal strategy. However, this example also highlights that the minimum of $\mathcal{F}$ at X is reached along a non-trivial curve that does not correspond to the global CPI constraint. In general, the possible maximum reduction of the cost function is given by $\mathcal{F}(N) - \mathcal{F}(X)$, and the performance η of a control that leads to a certain flow state Y shown in Fig. 2 c) can be expressed with respect to its potential, by computing the ratio between the realized reduction of $\mathcal{F}$ and the maximum possible reduction, i.e.

$$\eta = \frac{\mathcal{F}(N) - \mathcal{F}(Y)}{\mathcal{F}(N) - \mathcal{F}(X)}.$$

3 Dimensionless Analysis

Here, we generalize the concept of the $E_t^* - U_b^{*-1}$ map by normalizing the both axes with appropriate hydrodynamics quantities. First, the horizontal axis can be easily made dimensionless by using $\nu^*/(U_b^* D^*) = Re_D^{-1}$, where Re_D is the diameter-based Reynolds number and ν^* is the fluid kinematic viscosity. To deal with the vertical axis, we first introduce an *effective* wall friction $\tau_w^{e\,*}$ based on the total power consumption $P_t^* = P_p^* + P_c^*$:

$$\tau_w^{e\,*} = \frac{P_t^*}{U_b^*} = \tau_w^* + \frac{P_c^*}{U_b^*}. \tag{3}$$

Employing Eq. (1), the total energy consumption E_t^* is obtained by simply replacing C_f with C_f^e as:

$$E_t^* = \frac{M^* {U_b^*}^2 C_f^e}{2A^*}, \tag{4}$$

where C_f^e is the effective friction coefficient defined in analogy to (2) as $C_f^e = 2\tau_w^{e\,*}/\rho^* {U_b^*}^2$.

Thus, the vertical axis may be interpreted as an effective friction coefficient:

$$C_f^e = \frac{2A^* E_t^*}{M^* {U_b^*}^2}. \tag{5}$$

and the plane described in Fig. 1 (b) becomes analogous to the conventional $C_f - Re$ plane, with the added benefit of including the energetic cost of the control. However, like in the usual $C_f - Re$ plane, the above form is still not suitable for the present purpose, since the measure of convenience, i.e., U_b^*, appears explicitly in the denominator of C_f^e. In order to avoid this, multiplication of Eq.(5) with Re_D^2 results in:

$$C_f^e Re_D^2 = \frac{2A^* E_t^*}{M^* (\nu^*/D^*)^2}. \tag{6}$$

This way, E_t^* is non-dimensionalized by the fluid viscosity and geometrical properties of the duct only.

Fig. 3(a, b) graphically illustrates the non-dimensional form of Fig. 1 (a, b) with isolines of a typical cost function given by a quadric sum of energy expenditure and inconvenience:

$$\mathcal{F} = \left(\frac{C_f Re_m^2}{\alpha}\right)^2 + \left(\frac{Re_m^{-1}}{\beta}\right)^2, \tag{7}$$

where α and β is relative costs of energy expenditure and inconvenience. In this example, they are set to be $(\alpha, \beta) = (545312, 0.000198)$. We consider a fully developed turbulent channel flow, and the Reynolds number Re_m is defined based on the bulk mean velocity and the channel hight. The optimal operation condition of the uncontrolled flow is given by the red solid circle, where $\mathcal{F}$ is minimized on the black curve. This corresponds to the bulk Reynolds number of $Re_m = 6340$, which is equivalent to the Friction Reynolds number of $Re_\tau = 200$. As for a control technique, we consider spanwise wall oscillation (Jung et al., 1992), since it is one of the simplest open-loop control scheme, and also offers a large amount of available control results. Plotted in Fig. 3 are results obtained by Quadrio & Ricco (2004) and Ricco et al. (2012) under CFR and CPG, respectively.

In Fig. 3 (a), where the vertical axis represents the dimensionless pumping energy, significant pumping energy saving is confirmed under CFR, while enhancement of the convenience is achieved at the same pumping energy under CPG. Once the energy expenditure for flow control is taken into account, the overall picture changes drastically as shown in Fig. 3 (b). Namely, most controlled flow states are located above the uncontrolled turbulent line, indicating that the control modes consider here do not have advantage in the proposed energy-convenience map. This is because the present oscillation modes have relatively large amplitude of wall velocity, and therefore requires large

energy input. Taking a closer look, however, there is one blue cross which is below the uncontrolled turbulence line. This corresponds to the optimal oscillation mode, where the net energy saving rate of 7 % is obtained under CFR condition (Quadrio & Ricco, 2004).

In Fig. 3 (b), one point, marked with the black diamond, represents a new result, obtained in the present work, and corresponds to the CPI condition. To our knowledge, this is the first DNS ever carried out under such condition. The flow state is moved by the control action along the dash-dotted line drawn in Figs. 1 (b) and 2 (c). To achieve this, we have scanned through several combination of the oscillation parameters. For each of them, our numerical code computes runtime the control power required by the oscillating wall, and decreases the pumping power accordingly, so that their sum remains constant and equal to the pumping power of the non-controlled flow. The point in the figure represents the configuration that yields the maximum increase in the flow rate. Friction drag is reduced at the same time, and control power is naturally accounted for. Apart from the CPI strategy, this new set of simulations is identical to those by Quadrio & Ricco (2004), in terms of numerical scheme, value of Re, size of computational box and spatial resolution.

It is known that the oscillating wall is quite ineffective in producing net energy savings. Indeed, the lowest point in Fig. 3 (a) corresponds to a net energy saving of about 7%. At such small values, it is thus difficult to appreciate the quantitative difference between the best performance of the same technique with respect to the chosen cost function. The conceptual difference of the two points in the energy–convenience plane, however, is clearly established. We also note that more sophisticated control algorithms using streamwise traveling waves of spanwise wall motion (Quadrio et al., 2009), streamwise traveling wave of wall blowing/suction (Min et al., 2006, Hoeffner & Fukagata, 2009), and wall deformation (Nakanishi et al., 2012) have been proposed recently, and they generally achieve larger net energy saving rates when their control modes are properly optimized. The proposed energy-money plane provides a unique framework to compare control performances obtained under different control techniques and flow conditions.

4 Conclusions

The optimization problem of flow control involves an interplay between energy saving and convenience. Starting from this observation, a methodology for assessing flow control techniques for skin-friction drag reduction is proposed. We derive two dimensionless parameters, i.e., $C_f^e Re^2$ and Re^{-1}, which express the cost of the total energy consumption and the convenience for transporting a fluid through a duct with a certain cross-sectional geometry. Any controlled flow state can be represented in the two-dimensional plane composed by these two dimensionless quantities, without the need of imposing a constraint on the flow condition. The theoretical lower bound of the total energy consumption under a constant flow rate derived by Bewley (2009) and Fukagata et al. (2009) is naturally integrated into the plot.

The suggested "energy-convenience plane", which can also be used for external flows (see, Frohnapfel et al., 2012), extends the comparison of flow control techniques beyond the constant flow rate approach often used in literature up to now (Hoepffner & Fukagata, 2009, Kasagi et al., 2009), and allows the inclusion of application-specific cost functions such that the control performance can be judged in respect to a specific application.

Acknowledgments

The authors acknowledge support of projects FR2823/2-1 and 3-1 of the German Research Foundation (DFG) and the Cluster of Excellence"Center of Smart Interfaces" at TU Darmstadt. Yosuke Hasegawa gratefully acknowledges the support from the Japan Society for the Promotion of Science (JSPS) Postdoctoral Fellowship for Research Abroad.

References

Bewley, T. (2009), A fundamental limit on the balance of power in a transpiration-controlled channel flow, *J. Fluid Mech.*, Vol. 632, pp. 443-446.

Frohnapfel, B., Hasegawa, Y. & Quadrio, M. (2012), Money versus time: Evaluation of flow control in terms of Energy Consumption and Convenience. *J. Fluid Mech.* in press.

Fukagata, K., Sugiyama, K. & Kasagi, N. (2009), On the lower bound of net driving power in controlled duct flows, *Physica D*, Vol. 238, 1082?1086.

Jung, W. J., Mangiavacchi, N. & Akhavan, R. (1992), Suppression of turbulence in wall-bounded flows by high-frequency spanwise oscillations, *Phys. Fluids*, A4, 1605-1607.

Hoepffner, J. & Fukagata, K. (2009), Pumping or drag reduction? *J. Fluid Mech.* Vol. 635, 171?187.

Min, T., Kang, S.M., Speyer, J.L. & Kim, J. (2006), Sustained sub-laminar drag in a fully developed channel flow. *J. Fluid Mech.* Vol. 558, 309?318.

Nakanishi, H., Mamori, H. & Fukagata, K. (2012), Relaminarization of turbulent channel flow using traveling wave-like wall deformation, *Int. J. Heat Fluid Flow* in press.

Quadrio, M. & Ricco, P. (2004), Critical assessment of turbulent drag reduction through spanwise wall oscillation. *J. Fluid Mech.* Vol. 521, 251?271.

Quadrio, M., Ricco, P. & Viotti, C. (2009), Streamwise-traveling waves of spanwise wall velocity for turbulent drag reduction. *J. Fluid Mech.* Vol. 627, 161?178.

Ricco, P., Ottonelli, C., Hasegawa, Y. & Quadrio, M. (2012), Changes in turbulent dissipation in a channel flow with oscillating walls, *J. Fluid Mech.* in press.

Schlichting, H (1979), *Boundary-layer theory.* McGraw Hill. Inc.

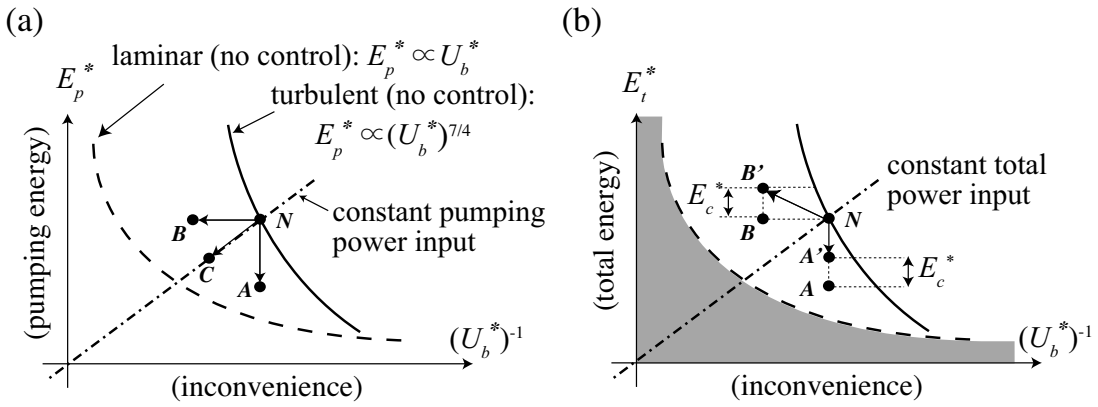

Figure 1: (a) Pumping energy E_p^* versus the inverse of the bulk mean velocity U_b^*, which reflects the time needed to pump a given amount of fluid through a duct with a given cross section and length. Starting from the non-controlled flow state N, successful flow control under CFR shifts it to A, whereas successful flow control under CPG shifts it to B. (b) Total energy E_t^* versus the inverse of the bulk mean velocity U_b^*. The vertical shifts from A and B in (a) to A' and B' represent the energy consumption E_c^* for the control.

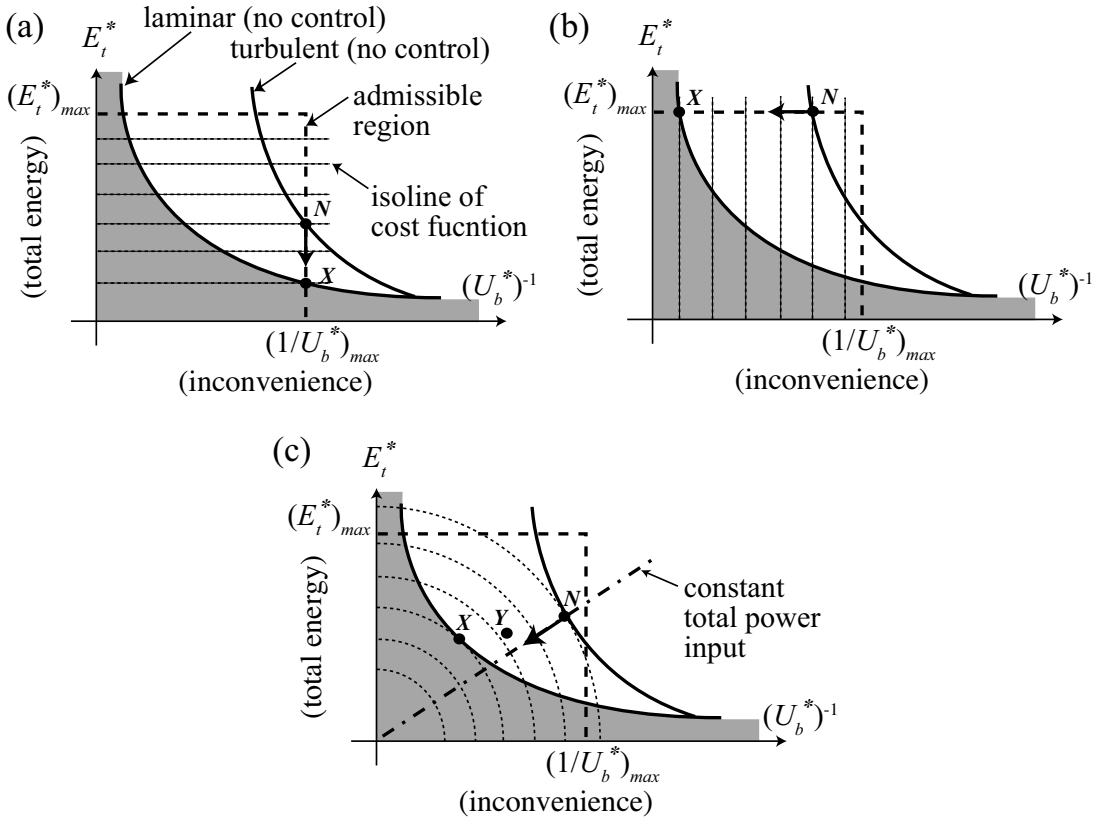

Figure 2: An energy-convenience plane with isolines of typical cost functions $\mathcal{F}$ represented by dotted lines; (a) $\mathcal{F} = E_t^*$, (b) $\mathcal{F} = 1/U_b^*$, (c) $\mathcal{F} = (E_t^*)^2 + (1/U_b^*)^2$. An admissible region defined by $(E_t^*)_{max}$ and $(1/U_b^*)_{max}$ affordable in the application is depicted by a square bounded by a dashed line. The flow state N is optimal for uncontrolled flow, while the laminar state X provides the minimum achievable value of the cost function by flow control.

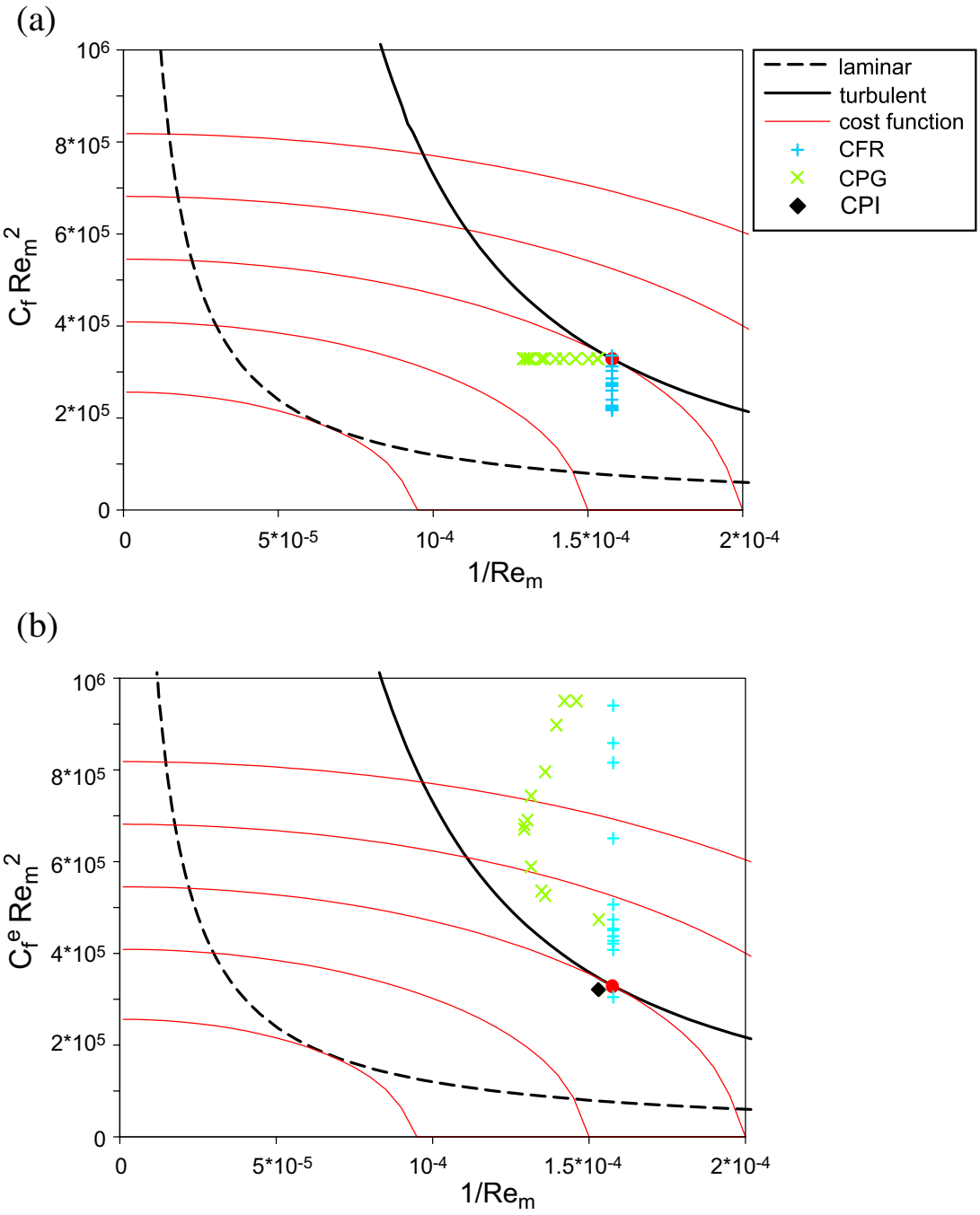

Figure 3: A nondimensional form of the suggested energy savings versus convenience planes of Fig. 1 (a) and (b), respectively. The vertical axis of (a) corresponds to the pumping energy, while that of (b) takes into account additional energy expenditure for flow control. The solid black line represents the Blasius correlation for the uncontrolled turbulent flow, while the black broken line shows the energy consumption of a laminar flow under a given flow rate, i.e., convenience. The red curves correspond to the iso-lines of the cost function given by Eq. (7). In this example, the red circle gives the minimum $\mathcal{F}$ in the uncontrolled flow (along the black solid line). Control results obtained by spanwise wall oscillation under CFR and CPG (Quadrio & Ricco, 2004, Ricco et al., 2012) are also plotted. The black diamond corresponds to a new data point obtained by the present CPI calculation.